

## Modeling of the GERDA data after the upgrade

M. MORELLA

*Gran Sasso Science Institute - L'Aquila, Italy*  
*INFN, Laboratori Nazionali del Gran Sasso - Assergi (AQ), Italy*

received 31 January 2022

**Summary.** — GERDA was an experiment at the Gran Sasso underground laboratories searching for neutrinoless double-beta decay of  $^{76}\text{Ge}$ . During 2018 the apparatus was upgraded, introducing possible new sources of contamination. A background model of the full-range energy spectrum acquired by germanium detectors before applying high level cuts (Pulse Shape Discrimination and LAr veto) after the upgrade is reported. From this analysis it is possible to understand the origin of the collected events, make a precise measurement of the half-life of the Standard Model allowed two neutrino decay mode and obtain information about the purity of the materials for future experiments' strategies.

### 1. – Introduction

Neutrinoless double-beta decay ( $0\nu\beta\beta$ ) [1] is a second-order weak process and consists in the  $\beta$  decay of two neutrons (protons) into two protons (neutrons) without the emission of neutrinos in the final state:

$$(1a) \quad \beta^-\beta^-: \quad N(A, Z) \rightarrow N(A, Z + 2) + 2e^-,$$

$$(1b) \quad \beta^+\beta^+: \quad N(A, Z) \rightarrow N(A, Z - 2) + 2e^+.$$

Transitions that could occur through  $0\nu\beta^+\beta^+$  could also occur through single ( $0\nu\text{EC}\beta$ ) or double ( $0\nu\text{ECEC}$ ) electron capture.

Differently from standard double beta decay  $2\nu\beta\beta$  (which is allowed and was observed in about ten different nuclei),  $0\nu\beta\beta$  is not allowed in the SM and it has never been observed so far. This process would violate the B-L symmetry (difference between baryon and lepton numbers), which is the truly conserved global symmetry in SM. Moreover, for this decay to happen, neutrinos have to be Majorana particles (*i.e.*, a particle that coincides with its antiparticle). The experimental signature of  $0\nu\beta\beta$  is a monoenergetic peak at an energy equal to the  $Q$ -value of the reaction.

The neutrinoless double-beta decay half-life can be factorized as follows [2]:

$$(2) \quad \left[T_{1/2}^{0\nu}\right]^{-1} = G_{0\nu} |M_{0\nu}|^2 |\langle\eta\rangle|^2.$$

$G_{0\nu}$  is the phase space factor and it is computed by integrating over all the possible final states involving the emitted leptons;  $M_{0\nu}$  is the nuclear matrix element and it contains information about the nuclear physics of the transition between initial and final state nuclei and  $\langle\eta\rangle$  is the new physics term responsible for the neutrinoless decay. In the standard interpretation scenario (exchange of light Majorana neutrinos)

$$(3) \quad \langle\eta\rangle = \frac{\langle m_{\beta\beta} \rangle}{m_e^2} = \sum_{i=1}^3 \frac{U_{1i}^2 m_i}{m_e^2} = \frac{c_{12}^2 c_{13}^2 m_1 + s_{12}^2 c_{13}^2 e^{i\gamma_1} m_2 + s_{13}^2 e^{i\gamma_2} m_3}{m_e^2},$$

where  $\langle m_{\beta\beta} \rangle$  is called effective Majorana mass and it is the sum of neutrinos mass eigenvalues weighted with the first row coefficients of the PMNS mixing matrix. By measuring  $T_{1/2}^{0\nu}$  it is possible to compute the effective Majorana mass term and have an indirect information on neutrino masses and neutrinos mass hierarchy (or ordering).

## 2. – The GERDA experiment

The GERDA experiment (GERmanium Detector Array) was devoted to the search of  $0\nu\beta\beta$  in  $^{76}\text{Ge}$  using High-Purity Germanium (HPGe) detectors. Since the isotopic fraction  $f_{76}$  of  $^{76}\text{Ge}$  in natural germanium is about 7.8%, the diodes were made of enriched material reaching a fraction of 86% or higher, thus acting as  $0\nu\beta\beta$  source and increasing the detection efficiency of the experiment. Operating enriched HPGe allowed the experiment to have great energy resolution ( $\sim 0.2\%$  at  $Q_{\beta\beta} = 2039 \text{ keV}$ ) [3, 4].

**2.1. GERDA Phase II setup.** – Ge detectors were arranged in 7 strings, for a total of 40 detectors, within a cryostat filled with  $64 \text{ m}^3$  of liquid argon (LAr). Each string was enclosed in a nylon mini-shroud to prevent  $^{42}\text{K}$  drifting in LAr and depositing on detectors' surface. One of the main feature of the experiment was operating bare germanium detectors directly in contact with LAr, resulting in a significant reduction of cladding material (and thus possible background sources). The cryostat was surrounded by a tank filled with ultra-pure water, acting as passive shield against external radiation and cosmic muon veto through Cherenkov light detection. Ge detectors were lowered into LAr using a lock system located in a clean room on top of the water tank. Another muon system (plastic scintillator) was placed on top of the clean room.

During GERDA Phase II three types of detectors were used: semi-coaxial (ANG and RG) enriched detectors, BEGe enriched detectors and natural semi-coaxial GTF detectors. All detectors were obtained from high-purity p-type germanium crystals. The  $n^+$  contact, where the external voltage is applied, was obtained by lithium diffusion ( $\sim 1 \text{ mm}$  thickness). The  $p^+$  electrode, where the signal is read out, was instead fabricated by boron implantation ( $\sim 100 \mu\text{m}$  thickness). Semi-coaxial detectors had a cylindrical shape and a bore-hole excavated along their axis where the  $p^+$  electrode was implanted. In this configuration relatively large sized detector could be manufactured (2–3 kg). Broad Energy Germanium (BEGe) detectors did not have a bore-hole and the  $p^+$  contact was a small, dot-shaped surface at the center of one of the two detector sides. The absence of a bore-hole makes this kind of detectors harder to electrically deplete; as a result they have smaller masses, generally lower than 1 kg.

**2.2. GERDA Phase II<sup>+</sup> upgrade.** – During Phase II the experiment was upgraded as a test bench for the next-generation experiment, LEGEND [5]. Post upgrade phase is referred to as Phase II<sup>+</sup>.

Natural germanium detectors were replaced by 5 enriched inverted-coaxial detectors placed in the central string, for a total of 41 detectors. They had a bore-hole like semi-coaxial, allowing large masses detectors, and a dot-shaped  $p^+$  electrode, obtaining PSD performance comparable with BEGe detectors. The LAr veto system was also improved by adding 50% more fibers around the array and a new fiber curtain was placed around the central string to enhance light detection probability in volume inside the detector array. All the previous nylon mini-shrouds were replaced with new ones fabricated from the same material.

### 3. – GERDA background model

Data were recorded using FADCs and then digitally processed off-line. The energy deposition associated to each germanium detector signal was determined via a zero area cusp (ZAC) filter [6] which was optimized off-line for each detector and each calibration. Calibrations were usually taken with three  $^{228}\text{Th}$  sources which were lowered into the LAr to the vicinity of the detector array in a 1–2 week cycle. Calibrated Ge detectors data were then used for the analysis, before applying high level cuts (such as LAr veto and Pulse Shape Discrimination).

By defining the multiplicity of an event as the number of germanium detectors in which an energy of at least 40 keV is registered, the dataset was divided into M1 (multiplicity one) and M2 (multiplicity two). M1 events were further split into 3 datasets according to the different detector geometries called M1-enrBEGe, M1-semiCoax and M1-invCoax. The energy in M2-enrAll events was the sum of the energy of the two germanium detectors triggered. The probability density functions (*pdf*'s) used to model contributions to the energy spectra were obtained from Monte Carlo simulations generated through the MAGE simulation framework [7], containing a software implementation of the GERDA PhaseII<sup>+</sup> experiment. Background events coming from contamination sources were simulated in and around the assembly. Materials close to the detectors were screened for radioactive contaminations originating from the  $^{238}\text{U}$  and  $^{232}\text{Th}$  decay chains,  $^{40}\text{K}$  and  $^{60}\text{Co}$ . These measurements were then used as prior distributions for background sources activities (see ref. [4], sect. 5).

The multivariate statistical analysis, used to model and disentangle the background in its components, ran on four binned datasets: M1-enrBEGe, M1-semiCoax, M1-invCoax and M2-enrAll. Assuming that the number of events in each bin follows a Poisson distribution, the complete likelihood function reads [8]

$$(4) \quad \mathcal{L}(\lambda_1, \dots, \lambda_m | \text{data}) = \prod_{d=1}^{N_{dat}} \prod_{i=1}^{N_{bins}} \text{Pois}(n_{d,i}; \nu_{d,i}),$$

where  $n_i$  is the experimental number of counts in the  $i$ -th bin and  $\nu_i$  the expected one;  $\lambda_i$  are the parameters of interest (contaminants activities,  $0\nu\beta\beta$  half-life). To obtain posterior probabilities for  $\lambda_i$ , the likelihood function is multiplied according to the Bayes theorem by a factor modeling the prior knowledge of each background component (screening measurements).

### 4. – Results

The final full range model (see fig. 1 for inverted-coaxial geometry result) consisted of 16 parameters, chosen according to screening measurements (if available) and activities'

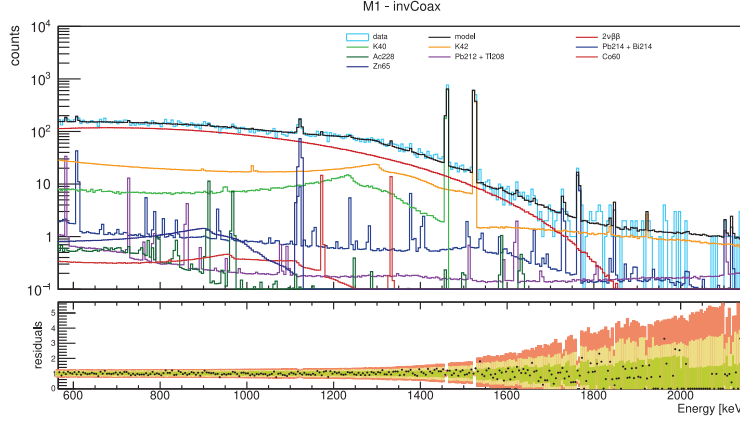


Fig. 1. – Global model fit results with residuals of using single detector events coming from new geometry detectors (inverted-coaxial). The fit range is [565, 2150] keV. Contributions from the same isotope coming from different locations in the setup are summed together. In the bottom plot, the data-to-model ratio is shown together with smallest 68%, 95% and 99% confidence intervals.

TABLE I. – *Background Index (BI) at  $Q_{\beta\beta}$  prior active background suppression in units of  $10^{-3}$  cts/(keV·kg·yr).*

	M1-enrBEGe	M1-semiCoax	M1-invCoax
PhaseII <sup>+</sup>	12	8.0	28
PhaseII [8]	$16.04^{+0.78}_{-0.85}$ (stat)	$14.68^{+0.47}_{-0.52}$ (stat)	–

posterior distributions (nuclei with *pdf*'s peaked at zero were removed). Background Indices (BIs) prior active background reduction for each detector type were extracted from parameters posterior distributions for each isotope/location combination (see table I for a summary). PhaseII<sup>+</sup> values (divided by dataset) were in agreement with PhaseII estimates. Most important contributions to BIs are <sup>208</sup>Tl and <sup>214</sup>Bi located in signal and HV cables for BEGe and semi-coaxial detectors. The greatest BI contribution for inverted-coaxial detector came from <sup>42</sup>K on their n<sup>+</sup> contact because of more ions drifting in LAr towards the central string, where these detectors were placed, resulting in a higher total BI prior active cuts with respect to the other strings in the array.

## REFERENCES

- [1] FURRY W. H., *Phys. Rev.*, **56** (1939) 1184.
- [2] GIUNTI C. *et al.*, *Fundamentals of Neutrino Physics and Astrophysics* (Oxford University Press) 2007.
- [3] ACKERMANN K. H. *et al.*, *Eur. Phys. J. C*, **73** (2013) 2330.
- [4] AGOSTINI M. *et al.*, *Eur. Phys. J. C*, **78** (2018) 388.
- [5] ABGRALL N. *et al.*, arXiv:2107.11462 (2021).
- [6] AGOSTINI M. *et al.*, *Eur. Phys. J. C*, **75** (2015) 255.
- [7] BOSWELL M. *et al.*, *IEEE Trans. Nucl. Sci.*, **58** (2011) 1212.
- [8] AGOSTINI M. *et al.*, *J. High Energy Phys.*, **2020** (2020) 139.